Bulk metallic glasses

2001 J. Phys.: Condens. Matter 13 7723

(http://iopscience.iop.org/0953-8984/13/34/316)

INSTITUTE OF PHYSICS PUBLISHING JOURNAL OF PHYSICS: CONDENSED MATTER

J. Phys.: Condens. Matter **13** (2001) 7723–7736 PII: S0953-8984(01)25895-0

Bulk metallic glasses

Susanne Schneider

I. Physikalisches Institut der Universität Göttingen, Bunsenstraße 9, 37073 Göttingen, Germany

E-mail: susanne.schneider@physik.uni-goettingen.de

Received 19 June 2001
Published 9 August 2001
Online at stacks.iop.org/JPhysCM/13/7723

Abstract

A recently developed large number of bulk glass-forming alloys, known as bulk metallic glasses, offer new opportunities for engineering applications and basic research on the nature of the glassy and undercooled liquid states in metals. This text gives a short review on bulk metallic glasses and their properties, focusing on the Vitreloy™ alloys which belong to the best-investigated group of bulk glass-forming metallic systems.

1. Introduction

When a liquid is cooled down below its melting temperature, T_m, either crystallization or undercooling may occur. During the latter process, homogeneous nucleation of crystalline phases is suppressed for an extended period of time. If the cooling rate is sufficiently high, homogeneous nucleation of crystalline phases can be completely avoided. Then, with decreasing temperature, the undercooled liquid becomes more and more viscous and finally falls out of equilibrium into the structurally arrested glassy state. Microscopically, the glassy state is characterized by a lack of long-range atomic order and is very similar to a frozen-in liquid.

The crystallization event, as a first-order phase transition, exhibits a pronounced discontinuity at T_m of the extensive physical properties such as volume, V, entropy, S, and enthalpy, H. In contrast, the undercooled liquid state is characterized by a continuous change of these thermodynamic variables from 'liquid-like' to 'solid-like' values. Usually, at the glass transition temperature, T_g, changes in the slopes of the $V(T)$, $S(T)$, and $H(T)$ curves occur, and can be experimentally observed as discontinuities in the thermal expansion, compressibility, or heat capacity versus temperature curves. The value of the experimentally determined glass transition temperature depends on the thermal history of the system and on the timescale of the measurement. It e.g. decreases with decreasing cooling rate during sample preparation or increasing timescale of the experiment. This indicates that the glass transition is dominated by kinetics, if not a purely kinetic phenomenon. Besides the non-thermodynamic point of view, discussion on an underlying thermodynamic phase transition based on entropy and free-volume theory is still going on.

0953-8984/01/347723+14$30.00

Glass formers are known in all major bonding classes: covalent, ionic, van der Waals, hydrogen bond, and metallic. Among these the metals generally require the highest cooling rates for complete vitrification. This has been attributed to the isotropic character of the metallic bonding. Formation of metallic glasses by cooling the melt was discovered by Klement *et al* [1] in 1960 when they applied rapid-solidification methods to the $Au_{75}Si_{25}$ metallic alloy melt[1]. The 'conventional' (mostly binary) metallic glass-forming alloys must be rapidly quenched with rates up to 10^6 K s^{-1} for vitrification. The thickness of such samples is limited to the μm regime. More recently, a new family of glasses, the 'bulk metallic glasses' (BMG) has been found with much lower critical cooling rates of 100 K s^{-1} to 1 K s^{-1}. Closely related to these much lower cooling rates is a much higher critical thickness of up to several cm. These three-dimensional metallic glasses exhibit important mechanical properties, e.g. a high elastic strain limit of about 2%, no work hardening, and very small shrinkage during solidification. From the scientific viewpoint the increased sample thickness of BMG is beneficial, e.g. for neutron scattering or low-temperature specific heat experiments, which are mass-sensitive techniques. But the more important feature of BMG is their much higher thermal stability with respect to crystallization in the undercooled liquid state compared to conventional metallic glasses. This makes experimental investigations of the glass transition and the undercooled liquid state of a metallic system possible that were not feasible before. Although this is a major step towards the understanding of metallic glasses, the experimental opportunities are still limited compared to those for other glass-forming systems, such as oxide glasses or polymers.

2. Bulk metallic glasses

The earliest studies of bulk metallic glasses were reported on the Pd–Cu–Si, Au–Pb–Sb, and Pd–Ni–P alloys. Of these the Pd–Ni–P alloy can be prepared with dimensions up to 1 cm [3]. Preparation requires specific procedures (drop tube methods, fluxing techniques) to suppress heterogeneous nucleation at the sample surfaces. In addition, high costs of the pure elements make these alloys less appropriate for technical applications.

Beginning in 1990, Inoue and co-workers showed that Ln–Al–LTM alloys (where Ln represents the major component, a lanthanide, and LTM a late transition metal) can be prepared in the fully glassy state by casting samples of dimensions of a few millimetres. Since then, a still increasing number of ternary, quaternary, and higher-order bulk glass-forming alloys have been reported by this group [4–11], illustrating that bulk glass formation is a far more general phenomenon than previously thought and not limited to just a few very special alloys. In 1993, Peker and Johnson developed the family of Zr–Ti–Cu–Ni–Be glasses with significantly lower critical cooling rates down to 1 K s^{-1} and supercooled liquid regions up to 135 K. Among these alloys are $Zr_{41.2}Ti_{13.8}Cu_{12.5}Ni_{10}Be_{22.5}$ (Vit1) [12], at this time the best glass former in that particular system with the lowest critical cooling rate, and $Zr_{46.7}Ti_{8.3}Cu_{7.5}Ni_{10}Be_{27.5}$ (Vit4) with a larger supercooled liquid region but higher critical cooling rate than Vit1. Hays and Johnson are still exploring the Zr–Ti–Cu–Ni–Be phase diagram and have recently found the alloy $Zr_{45.4}Ti_{9.6}Cu_{8.6}Ni_{10.1}Be_{26.3}$ (Vit1c) with the largest known value, $T_x - T_g = 135$ K, at a heating rate of 20 K min^{-1}, found in DSC measurements for the width of the supercooled liquid region in all metallic systems (T_x: temperature of first crystallization event) [14]. Other systems developed in the Johnson group include Ti–Zr–Cu–Ni [13] and Zr–Nb–Cu–Ni–Al [15]. One particular member of the latter family of the Be-free alloys, $Zr_{58.5}Nb_{2.8}Cu_{15.6}Ni_{12.8}Al_{10.3}$ (Vit106a), reaches the glass-forming ability and width of the supercooled liquid region of

[1] A rather different approach of preparing non-crystalline metallic solids by condensation of elemental metal vapour onto cold substrates was reported in 1954 by Buckel and Hilsch [2].

Vit1 and, e.g., can be fully vitrified in an electrostatic levitator by free radiative cooling (see section 2.2.2) [15]. Most of the recently discovered BMG can be described as pseudo-ternary alloys of the composition $ETM_{100-x-y}LTM_xSM_y$, where ETM is a combination of early transition metals (Zr, Ti, Nb), LTM a combination of late transition metals (Cu, Ni, Co, Fe), and SM a simple metal element (Be, Mg, Al). The composition usually lies in a region of low liquidus temperatures, often close to deep eutectics, where the melt is stabilized with respect to the solid state and far from Laves phases in the system. In these alloys the high solubility of oxygen in zirconium and of carbon in beryllium hinders the homogeneous nucleation of oxide particles in the melt. Thus, heterogeneous nucleation of the intermetallic compounds triggered by these high-melting-temperature oxide particles is suppressed for an extended content of oxygen impurities.

2.1. Origins of the glass-forming ability

The glassy state is not the equilibrium state of solids. It can only be reached if the formation and growth of competing crystalline equilibrium phases can be avoided or at least significantly slowed down during preparation. For the case of glass preparation by cooling the melt, Turnbull has discussed the crystal nucleation and growth kinetics [16]. Using a simple nucleation theory [17] with typical metallic material parameters, he shows that the reduced glass transition temperature, $T_{rg} = T_g/T_m$, is a key parameter that determines whether or not the melt of a given material can form a glass during cooling. Assuming that the shear viscosity of the undercooled liquid, η, follows a Vogel–Fulcher–Tammann relation and the nucleation rate is proportional to $1/\eta$, he shows that the peak of the nucleation rate versus reduced temperature curve, $I(T_r)$, with $T_r = T/T_m$, lowers, sharpens, and shifts to higher T_r with increasing T_{rg}. For $T_{rg} \geqslant 2/3$ the I-values exceed the experimentally observable limit of 1 m^{-3} s^{-1} only slightly and in a relatively narrow temperature window around $0.7 \leqslant T_r \leqslant 0.8$. This temperature range can be passed sufficiently quickly during cooling that materials with $T_{rg} \geqslant 2/3$ should be good glass formers. The analysis also shows that the glass-forming ability increases with increasing shear viscosity at the melting point. Bulk metallic glasses have high T_{rg}-values [18] and the experimentally determined viscosities at the melting points of the Zr–Ti–Cu–Ni–Be glasses are 2–3 orders of magnitude higher than those of elemental metals or binary alloys at their respective melting points. Turnbull's analysis indicates how to find bulk metallic glass-forming systems: one should look for high values of T_{rg}. Since the glass transition temperature of a given material is in general not predictable and depends only slightly on composition, the search should focus on alloy compositions with low melting temperatures, i.e. where crystalline phases are relatively unstable with respect to the melt. In addition, the melt should have a significantly negative heat of mixing.

An effective way of 'designing' such an alloy is described by Johnson [18]: he suggests frustrating the tendency of an alloy to crystallize by introducing multiple chemically different atoms such that these atoms cannot arrange themselves into a simple crystalline structure. Such a simple crystalline structure would be associated with high atomic level strains, mainly arising from atomic size differences [19]. This forces the complexity and size of the unit cell to increase with increasing number of different species involved. In such alloys the free-enthalpy difference between the liquid and competing crystals is small, and thus the melting point is low. Johnson has consequently followed [18] this 'confusion principle' [20]. He started by looking for binary alloys with deep eutectics (Zr–Be, Ti–Be) and successfully added suitable additional components (Cu, Ni) to lower the eutectic temperatures even more. With his strategy he developed some of the best bulk glass-forming metallic alloys known today, with compositions close to eutectic ones.

The three empirical rules framed by Inoue *et al* [21] accord with the above. They suggest that bulk amorphous alloys can be formed by multicomponent systems with (1) more than three components, (2) atomic size differences between the main constituents of more than 12%, and (3) negative heats of mixing between the constituents. These rules are based on a number of bulk glass-forming alloys successfully developed by these authors [4–11].

Desre *et al* have performed a thermodynamic analysis of the glass-formation ability of multicomponent liquids. They calculate the homogeneous nucleation rate in a multicomponent alloy with a negative heat of mixing and find that the addition of one more component can reduce the probability for a concentration fluctuation leading to the formation of a critical nucleus by an order of magnitude [22, 23]. Furthermore, they argue that the addition of components to a glass-forming system that are strongly interacting with each other but weakly with the components of the parent phase can increase the liquid–crystal interface energy and thus the energy barrier for nucleation [24].

2.2. Thermophysical properties

The most systematic and complete studies of BMG have been performed by Johnson and co-workers on Zr–Ti–Cu–Ni–Be glasses. This text will mostly be restricted to experimental results on thermophysical properties of this 'Vitreloy™' alloy family. It is assumed that the results to be reported are representative for all BMG. For convenience, different alloy compositions will be referred to by the abbreviations listed in table 1. In addition, glass transition and crystallization temperatures, as derived from differential scanning calorimetry (DSC) measurements, are shown. Since both temperatures depend on the DSC heating rate [25, 26], the respective rates are indicated. The width of the supercooled liquid region, $T_x - T_g$, is a convenient measure of the stability of the undercooled liquid with respect to crystallization upon heating.

Table 1. Bulk metallic glass-forming alloys, their glass transition and crystallization temperatures (first crystallization event), T_g and T_x, as derived from DSC experiments, the respective DSC heating rates, and their abbreviations as used in this text.

Alloy composition (at.%)	T_g (K)	T_x (K)	Heating rate (K min^{-1})	Abbreviation
$(Zr_{75}Ti_{25})_{55}(Cu_{55}Ni_{45})_{22.5}Be_{22.5}$	610	710	20	Vit1 [14]
$(Zr_{77.5}Ti_{22.5})_{55}(Cu_{52}Ni_{48})_{21.25}Be_{23.75}$	620	705	20	Vit1a [14]
$(Zr_{80}Ti_{20})_{55}(Cu_{49}Ni_{51})_{20}Be_{25}$	602	730	20	Vit1b [14]
$(Zr_{82.5}Ti_{17.5})_{55}(Cu_{54}Ni_{46})_{18.75}Be_{26.25}$	625	760	20	Vit1c [14]
$(Zr_{85}Ti_{15})_{55}(Cu_{43}Ni_{57})_{17.5}Be_{27.5}$	620	750	20	Vit4 [14]
$Zr_{58.5}Nb_{2.8}Cu_{15.6}Ni_{12.8}Al_{10.3}$	674	772	20	Vit106a [15]

2.2.1. Thermodynamic functions. The thermodynamic functions can be derived from measurements of the temperature-dependent specific heat capacity difference, $\Delta c_p(T)$, between the undercooled liquid and the crystalline state. As shown in [26–28], Vit1 and other multicomponent glass-forming alloys exhibit an endothermal heat effect at the glass transition temperature, T_g. The increase in the heat capacity at T_g of the metallic glass of typically 20 J mol^{-1} K^{-1} appears small compared to those of simple ionic or van der Waals bonded liquids but is still higher than for example that in the highly coordinated network SiO_2. The Gibbs free-energy difference between the crystal and the supercooled liquid, as calculated from the $\Delta c_p(T)$ data, is relatively small compared to, for example, that of binary metallic glass-forming systems [28]. The small driving force for nucleation in the undercooled liquid

is one likely reason for the good glass-forming ability of these alloys. Similarly, the change in configurational entropy and enthalpy in the supercooled liquid is small. In the framework of Angell's fragility concept (see section 2.2.3), BMG are relatively 'strong' glasses. The investigations show further that T_g and the crystallization temperature, T_x, strongly depend on the heating rates like in many non-metallic glasses.

With the knowledge of the changes of specific heat capacity, Δc_p, thermal expansion coefficient, $\Delta\alpha_p$ [29], and isothermal compressibility, $\Delta\kappa$, at T_g, the Prigogine–Defay ratio, $\mathrm{PD} = (\Delta\kappa\,\Delta c_p)/(T_g V(\Delta\alpha_p)^2)$, for Vitreloy alloys was calculated [30]. It is greater than unity and compares to values known for non-metallic systems.

2.2.2. Time–temperature transformation diagrams. The majority of BMG known today are Zr- or Ti-based systems. As such they are highly reactive in the liquid or undercooled liquid states and tend to chemically attack almost all crucible materials. This may give rise to composition changes of the liquid and/or heterogeneous nucleation of crystalline phases. To study crystallization kinetics of BMG in detail, containerless processing and examination under high-vacuum conditions is desirable. The high-vacuum electrostatic levitator (HVESL) method developed by Rhim *et al* [31] provides a unique tool for such studies. In contrast to high-frequency electromagnetic levitation, the ESL technique decouples specimen heating and levitation. This permits annealing procedures with well controlled time–temperature profiles.

Using the HVESL technique, Kim *et al* were able to record a time–temperature transformation (TTT) diagram for Vit1 down to temperatures well below the crystallization 'nose' [32]. This is the first determination of the TTT diagram of a metallic glass former. The lowest temperature achievable was limited by the pyrometer employed for temperature measurement. Although the TTT diagram exhibits the expected 'C' shape, the authors were not able to explain the diagram using existing models that assume polymorphic crystallization. Later, Masuhr *et al* suggested a description using an effective diffusivity that scales with the viscosity at high temperatures and is Arrhenius-like in the supercooled liquid state (SLS) [33]. Besides Vit1, the only BMG known today whose TTT diagram can be determined over the whole range of the undercooled liquid by the HVESL technique is Vit106a [15].

Although most experimental investigations of BMG start from the glassy state and access the target temperature by heating, the TTT diagram provides a useful guideline for processing BMG or the accessible time window in isothermal experiments. The location of the crystallization 'nose' of Vit1, e.g., is consistent with the experimentally observed critical cooling rate, and the time available at a particular temperature for isothermal diffusion annealing of Vit4 without crystallization is not very different from the TTT diagram value [34].

Later, Masuhr *et al* demonstrated that clean high-purity graphite crucibles can be used for high-temperature studies of Vit1 [35, 36]. The liquid infiltrates the porous graphite crucible and forms a Zr–C reaction layer with a width of about 500 nm. No difference between the TTT diagrams measured in the HVESL set-up and in inductively heated graphite crucibles was detected [37, 38]. This indicates that the crystalline Zr–C layer is not promoting heterogeneous nucleation and the composition changes resulting from the carbide formation are not significant. Using graphite crucibles, the low-temperature branch of the TTT diagram of Vit1 could be measured down to about 600 K. This was possible because temperature measurement could be performed using a thermocouple.

In view of this surprising observation that there is no difference between the TTT diagrams derived from containerless levitation experiments and those measured in graphite crucibles, Schroers *et al* performed detailed studies of the microstructure after isothermal crystallization of Vit1 at different degrees of undercooling [37, 38]. Using graphite crucibles they observe a decrease of the typical length scales for nucleation by five orders of magnitude upon

lowering the temperature from 958 K to 613 K. Simultaneously the density of crystalline nuclei increases by fifteen orders of magnitude. This high density indicates a high nucleation rate and contradicts the prediction of a sluggish crystallization kinetics suggested by the low-temperature tail of the TTT diagram of Vit1. Schroers *et al* qualitatively explain this apparent contradiction as due to decomposition in the liquid state prior to crystallization (see section 3).

2.2.3. Shear viscosity of the undercooled liquid. Viscosity is a key parameter not only in Turnbull's nucleation theory (section 2.1) but also in Angell's fragility concept for liquids [39] and the free-volume [40] and mode-coupling theories [41]. Viscosity is proportional to the structural relaxation time, τ, of the liquid, $\eta = G_\infty \tau$ (G_∞ is the instantaneous shear modulus) and thus a macroscopic probe for microscopic processes. The temperature dependence of viscosity is important for processing and shaping by mould casting. Therefore, experimental data on the shear viscosity of undercooled metallic liquids are highly desired but were not available before the development of BMG. The significantly enhanced thermal stability of the new systems in the SLS made equilibrium viscosity measurements possible on timescales between several hours and some ten seconds at temperatures up to 100 K above the glass transition and in the vicinity of the melting point as well.

The first viscosity study on BMG was reported by Bakke *et al* [43]. This article reports the shear viscosity of Vit4 in the vicinity of the glass transition using parallel-plate rheometry. These data were supplemented by bending beam measurement in the same temperature regime [44] and can be described well with the Vogel–Fulcher–Tammann (VFT) relation, $\eta(T) = \eta_0 \exp[BT_0/(T - T_0)]$, with B a parameter related to the fragility (see below) and T_0 the VFT temperature [42]. Although for Vit1 the experimental timescale is limited by a chemical decomposition process with subsequent nanocrystallization, viscosity data were recorded both in the SLS and the equilibrium melt and slightly undercooled liquid [45]. The high-temperature rheological properties were measured in a high-temperature Couette viscosimeter. The combined viscosity data extend over a range of fourteen orders in magnitude and can be very well described by free-volume theory using the expression for the temperature-dependent free volume suggested by Grest and Cohen [46].

The viscosity of Vit1 at the liquidus temperature is three orders of magnitude larger than for simple metallic systems. This reflects a sluggish kinetics that significantly contributes to the glass-forming ability of this alloy, in accordance with Turnbull's analysis (section 2.1). In addition, the average free volume per atom resulting from the best-fitting parameters is small and supports the picture of a dense metallic liquid with a sluggish kinetics. In accordance with this, studies of the specific volume of Vit1 performed by Ohsaka *et al* in the HVESL show a negative excess volume over the ideal volume of the liquid [29].

Viscosity data are often used to classify glass-forming liquids according to the temperature dependence of their viscosities [39, 47]. A small number of 'strong' glass-forming liquids reveal Arrhenius behaviour of the viscosity, $\eta(T) = \eta_0 \exp[Q/k_B T]$, while all others show varying degrees of deviation from Arrhenius behaviour, and can be described by the VFT equation. The degree of deviation is called fragility and quantified by the slope, m, of the $\log_{10} \eta(T)$ versus T_g/T curve at T_g. The fragility is related to B through $m = BT_g/[(T_g - T_0)^2 \ln 10]$. Strong liquids have low values (around 20) and fragile liquids high values (around 100) of the fragility parameter m. Strong liquids like SiO_2 retain their short- and intermediate-range structural order when heated across the glass transition, while in fragile liquids like o-terphenyl the structural order rapidly changes with increasing temperature. Fragile liquids show relatively large changes in heat capacity and thermal expansion coefficient at T_g, and their viscosity decreases more rapidly with increasing temperature than that of strong glasses [48]. Perera has collected fragility parameter values for a number of ternary, quaternary,

and quinary glass-forming alloys [49]. He identifies the BMG as intermediate glass formers with an average fragility parameter of some 50 and finds a tendency of decreasing fragility with increasing number of components. Since the glass-forming ability increases with increasing number of components, this means a positive correlation between good glass-forming ability and 'stronger' behaviour of the undercooled liquid as discussed by the Johnson group [50, 51].

2.2.4. Atomic diffusion. Like viscosity, the atomic diffusion is closely linked to relaxation processes, and theories of the (undercooled) liquid state yield certain predictions about diffusion mechanisms that can be checked by careful measurement of e.g. the temperature or mass dependence of atomic diffusion. Atomic diffusion experiments on Zr–Ti–Cu–Ni–Be BMG have been performed well below (500 K–730 K) and above (1000 K–1200 K) the crystallization 'nose' temperatures (see section 2.2.2). Experiments at temperatures in between are prevented by the fast-crystallization kinetics in the vicinity of the 'nose' temperature. Most diffusion studies focus on the possible influence of the glass transition on the diffusivities and the diffusion mechanisms.

The first studies of atomic diffusion in the glassy and supercooled liquid states (SLS) of a BMG were reported by Geyer *et al* [52]. We have performed interdiffusion experiments on Be and Vit1 [52] and Vit4 [53] around the glass transition temperature, employing the elastic backscattering technique (EBS) [54] for depth profiling. This work has initiated numerous other investigations.

In the case of Vit1 only comparatively short diffusion anneals are feasible because this alloy undergoes a decomposition which acts as a precursor to crystallization and strongly influences the measured apparent diffusivities. This decomposition and subsequent crystallization was discovered in the course of diffusion experiments and will be discussed in detail in section 3. Since the evolution of the decomposition amplitude is very slow in the initial stages, annealing must be limited to short times such that undistorted diffusion profiles can only be obtained for sufficiently fast diffusants (like Be) before effects of decomposition become significant [55].

Vit4 is better suited for diffusion experiments since according to the investigations discussed in section 3 it does not show decomposition in the glass transition temperature regime. The temperature dependence of diffusion in Vit4 has been measured for a variety of elements at temperatures up to 730 K: Be [53], B, Fe, Al [55], Co [56], Ni, and Zr [34]. The temperature dependence of all diffusion data for the SLS is of the Arrhenius type with relatively high apparent activation energies. A possible explanation of these high values is given in [52]. In many cases, the diffusivities in the glassy state are higher than expected from the extrapolation of the Arrhenius behaviour in the undercooled liquid down to lower temperatures, and the low-temperature data can be fitted with a second Arrhenius law giving a lower activation enthalpy and resulting in a kink in the Arrhenius plot. In the case of Al, B, Fe, Co, and Ni the kink seems to result from insufficient relaxation of the samples [34].

However, in the case of Be diffusion it has recently been postulated that the low-temperature diffusion behaviour is an intrinsic property of the relaxed glassy state, and single-atom Be hopping involving thermal fluctuations of the spread-out free volume contributes to diffusion both below and above the kink temperature [57]. In a recent NMR investigation [58] no kinks are observed in the Arrhenius plots of the Be hopping rate, Ω, in Vit1 and Vit4 versus temperature. The measured activation energies and the difference between the hopping rates in Vit1 and Vit4 agree with the interdiffusion data for the glassy state. The measured hopping rates in the SLS surprisingly show the same Arrhenius behaviours as those below 625 K in both Vit1 and Vit4. The authors suggest a change of the diffusion mechanism: at low temperatures single-atom hopping dominates, while in the SLS it is cooperative motion of a group of several atoms.

Such cooperative atomic motion has been indicated by the isotope effect of cobalt (^{57}Co/^{60}Co) diffusion in Vit4 [56] and in $Zr_{65}Cu_{17.5}Ni_{10}Al_{7.5}$ [59]. The isotope effect values for the supercooled liquids are independent of temperature and almost vanish for both alloys. The average value is $E = 0.1 \pm 0.02$ in the case of Vit4 and $E = 0.075 \pm 0.04$ in the case of $Zr_{65}Cu_{17.5}Ni_{10}Al_{7.5}$. These values agree with those that have been obtained for relaxed conventional metallic glasses [60] and attributed to a highly cooperative hopping mechanism. This interpretation is consistent with molecular dynamics simulations of supercooled liquids in which stringlike or chainlike displacements of groups of atoms are observed [61–63]. From the measured isotope effects, some ten cooperatively moving atoms can be estimated.

Given these results and their consistency with mode-coupling theory (MCT) and molecular dynamics simulations, the predominance of a single-atomic jump mechanism at lower temperatures, as suggested by the NMR data, is surprising. Mode-coupling theory has been successfully applied to interpret the dynamics of several fragile non-metallic glass-forming systems. It predicts that below a critical temperature, T_c, liquid-like diffusion ('viscous flow') freezes out and diffusion is a medium-assisted highly cooperative hopping process, where whole clusters of atoms perform thermally activated transitions into new configurations. Since the experimentally determined critical temperature of Vit4 is well above the glass transition regime ($T_c = 875$ K $\pm$ 6 K [64]), one would expect only cooperative atomic motion of Be atoms. This problem needs further clarification.

For ^{63}Ni diffusion in Vit4 the pressure dependence has been measured and reveals the activation volume, ΔV, for Ni diffusion in the supercooled liquid [34]. ΔV is only slightly temperature dependent in the temperature interval analysed, if at all, and averages about 1.2 mean atomic volumes. Since the diffusion mechanism is most probably the same for Co and Ni in Vit4 (due to their similarity in size and chemistry), the measured activation volume for ^{63}Ni is most probably not the allocation of fluctuating 'free' volume to a single localized defect but is smeared out over all atoms that participate in the collective jump.

For Vit4 the atomic transport in the equilibrium melt above the liquidus temperature, $T_{liq} = 1050$ K, and at moderate undercoolings has been studied by means of quasi-elastic neutron scattering (QENS) [64]. The high-frequency dynamics of this alloy has been found to be in accordance with the scenario predicted by MCT [65]. Unfortunately the temperature regime around T_c is not experimentally accessible for diffusion experiments on the Zr–Ti–Cu–Ni–Be alloys with the result that e.g. data on the isotope effect of diffusion are not available. All available tracer diffusion data have been gained at temperatures far below this value. From the QENS data, average diffusivities of all constituents in the melt of Vit4 have been determined [64]. Their temperature dependence is much weaker than in the supercooled liquid and follows the MCT prediction for $T > T_c$, $D(T) \propto (T - T_c)^\gamma$ with $\gamma = 1.71$. However, an independent analysis of the neutron scattering data yields $\gamma = 2.65$ [64]. The expression $D \propto T^n$ which is sometimes discussed for diffusivity in liquids, with n close to 2 [66], can probably be excluded already on the basis of the available data since this formula would give a wrong curvature in the Arrhenius plot. It is interesting to note that the Stokes–Einstein relation between the diffusivity, D, and viscosity η, $D\eta = k_B T/6\pi r$ (r is the molecular radius), fails to hold for Vit4, both at temperatures around T_g [53] and at T_{liq} [64].

2.3. Mechanical properties of bulk metallic glasses

It has always been assumed that, due to the absence of a dislocation mechanism for plastic deformation and crack propagation, metallic glasses are high-strength materials. However, the high critical cooling rates required for preparation of conventional metallic glasses have limited the size of specimens for mechanical testing and for use in engineering applications.

In particular, specimens large enough for investigation of the dynamic constitutive behaviour of these materials were not available.

With the discovery of BMG, this limitation has been overcome and investigations on mechanical properties of BMG have been performed. In dynamic compression experiments on Vit1 an elastic strain limit of $\epsilon_c = 2\%$ and a yield stress of $\sigma_c = 1.8$ GPa (that is insensitive to strain rate) were measured [67]. These are extraordinarily high values, and the maximum elastic energy density, $U_{max} = \sigma_c \epsilon_c / 2$, that can be stored in Vit1 is extremely high. This makes Vit1 (and possibly other BMG as well) ideal for applications where plastic deformation is not desired. Among the first commercial products to utilize the high elastic yield are golf clubs [68].

In the case of Vit1, annealing in the vicinity of the glass temperature leads to a drastic reduction in fracture toughness such that the alloy behaves like a brittle ceramic [69]. This imposes a severe limitation for applications of these glasses at higher temperatures and is also important for procedures of shaping by mould casting. The origin of the embrittlement and deterioration of mechanical properties is the decomposition and nanocrystallization process discussed in section 3.

The benefits of the high elastic yield stress of the Zr–Ti–Cu–Ni–Be glasses are partly compensated by a relatively small plasticity [67]. Under tensile or compressive loading the samples fail catastrophically on one dominant shear band. Hays *et al* have produced an alloy that develops a two-phase microstructure which effectively modifies shear-band formation and propagation such that plastic strain to failure, impact resistance, and toughness are dramatically increased [70].

3. Decomposition and nanocrystallization of Vitreloy 1

According to Johnson's design rules (section 2.1), good glass-forming systems often have eutectic compositions. Since a eutectic alloy possesses an intrinsic tendency for phase separation it is not surprising that upon annealing a decomposition occurs in almost all Vitreloy alloys [72, 73]. This decomposition is a precursor for nanocrystallization and alters many properties of the glasses. The first indication of some kind of structural or chemical alteration during annealing was observed in Vit1 during atomic diffusion studies [52, 71]. The measured diffusivities became time dependent upon extended annealing, but at first wide-angle x-ray diffraction and transmission electron microscopy (TEM) did not show crystalline phases. To check for possible chemical alterations, small-angle neutron scattering experiments were performed and revealed a scattering contrast indicative of a chemical decomposition process [72]. The scattering curves, $S(Q)$, recorded after annealing at temperatures around the glass transition temperature show a correlation peak that grows with annealing time (figure 1). The correlation lengths, λ, estimated from the peak positions, Q_{max}, using $\lambda = 2\pi / Q_{max}$, are typically 10–50 nm.

At constant annealing temperatures the peak positions slightly shift to smaller Q-values with increasing annealing time. This process reveals two different time laws as indicated in figure 2 [73, 74]. The time-dependent second momentum, $S_2(t) = \int_0^\infty Q^2 S(Q, t)\, \mathrm{d}Q$, of the scattering curves shows a similar behaviour. The time dependence for both quantities changes at the transition time, t_x ($t_x(633\ \mathrm{K}) \approx 100$ min). This transition time decreases with increasing annealing temperature. High-resolution microstructural TEM studies of annealed samples reveal a high number density (about $10^{24}\ \mathrm{m}^{-3}$) of nanocrystals (typical diameter 2 nm) embedded in an amorphous matrix as soon as the annealing time exceeds t_x, while samples annealed for less than t_x are completely amorphous [73] (figure 3). The nanocrystals can also be detected by wide-angle x-ray diffraction after longer annealing times [73].

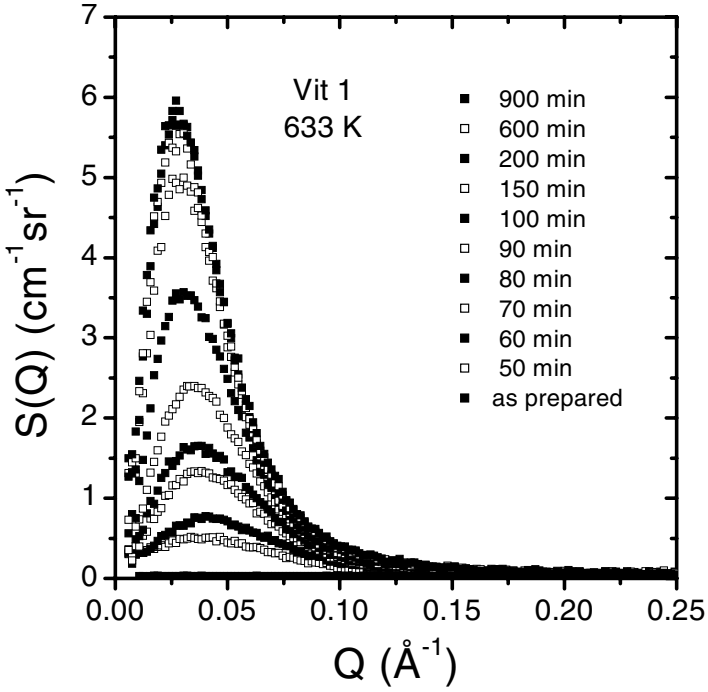

Figure 1. SANS data for the Vit1 alloy annealed at 613 K for different times.

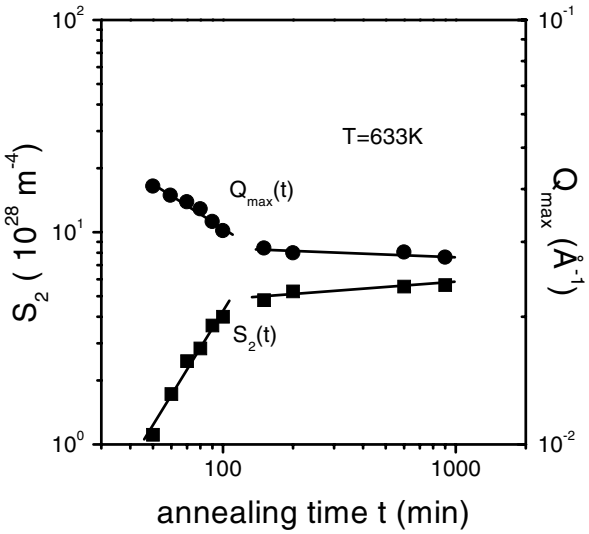

Figure 2. Values of Q_{max} and S_2 for SANS data on the Vit1 alloy annealed at 633 K for different times.

The results suggest that upon annealing the Vit1 alloy first undergoes a chemical decomposition leading to spatially correlated concentration fluctuations whose amplitude grows with annealing time. Accordingly, the local (composition-dependent) crystallization temperatures fluctuate. After the time t_x a critical amplitude is reached, such that T_x locally

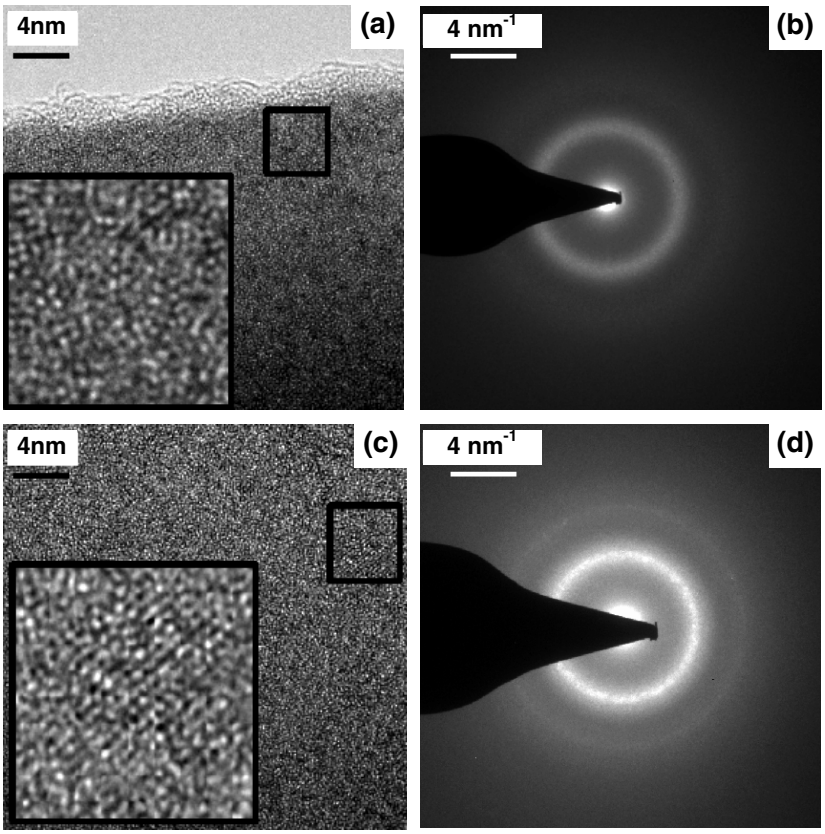

Figure 3. High-resolution TEM images of samples annealed at 633 K: after 60 min (a) and 600 min (c) of annealing, and corresponding small-area diffraction diagrams ((b), (d)). In (c), lattice fringes of a nanocrystal are visible, and the corresponding diffraction diagram (d) shows sharper rings than that in (b).

decreases below the annealing temperature and the sample abruptly begins to crystallize in a regular pattern that is determined by the correlation of the composition fluctuations. The small sizes of the nanocrystals and their high number densities result from the small correlation lengths. Once the nanocrystals exist, the alteration of the sample (further chemical redistribution, crystal growth) proceeds significantly more slowly.

The results of DSC measurement performed on Vit1 samples [72, 75] support the idea of continuous composition fluctuations ('composition waves'). They show a broad first crystallization event that is consistent with crystallization in a system with composition gradients and locally varying crystallization temperatures. According to the extent of formation of nanocrystals during isothermal annealing, the first crystallization peak of the as-prepared alloy disappears with increasing annealing time. Additionally, for the late stages, the glass transition in the non-crystallized regions broadens (as is expected in a compositionally inhomogeneous matrix) and its mid-point temperature shifts to higher values.

Recent SANS experiments on samples with contrast variation carried out by means of isotope substitution and anomalous small-angle x-ray scattering (ASAXS) show that Ti, Be, and Ni concentration fluctuations exist in the decomposed but still amorphous samples [73]. Compositional variations in the Zr content in as-prepared or decomposed samples, as

suggested by atom probe field-atom microscopy investigations [76], cannot be found by SAXS experiments. Only samples containing nanocrystals are inhomogeneous with respect to Zr. In particular, the Ti composition gradients are responsible for the SANS contrast because the average scattering length of the natural Ti isotope mixture is negative while all other elements have average positive scattering lengths. Thus, even a small Ti concentration variation causes a detectable scattering length density variation.

The positions $Q_{max}(t, T)$ of the correlation peaks are temperature dependent, and, when plotted as $Q_{max}(t_x, T)^2$ versus T, follow a straight line intersecting the temperature axis at a critical temperature, $T_c \approx 670$ K (figure 4).

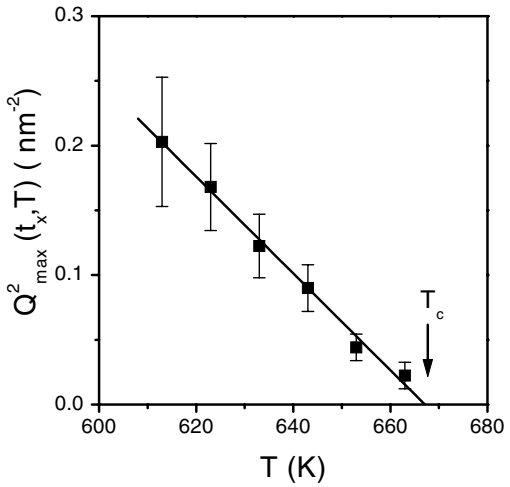

Figure 4. Correlation peak positions, Q^2_{max}, after annealing time t_x as a function of annealing temperature, T.

The existence of a correlation peak and the temperature dependence of its position have led to proposals that the decomposition process observed in Vit1 is of the spinodal type [77,78]. However, this point is still under discussion and alternative mechanisms have been proposed [79, 80]. The theory for early stages of spinodal decomposition developed by Cahn and Hilliard [77,78] is not consistent with the Vit1 data. Already the coarsening resulting in the slight time dependence of the peak positions cannot be described by this theory. Furthermore, the Q-dependent growth rate suggested by Cahn and Hilliard (postulating negative values for $Q > \sqrt{2}Q_{max}$) cannot be observed, so attempts to derive diffusion coefficients from the time dependence of the scattering data that are based on this theory [81] must be treated with caution.

At room temperature, the BMG Vit1 is located inside a miscibility gap in the quinary phase diagram. According to the SANS results, this gap extends up to 670 K at the Vit1 composition (figure 3). By changing the composition, the alloy changes its position inside the miscibility gap and can even leave the gap at room temperature. This has been demonstrated by SANS experiments on samples with different Ti:Be composition ratios [82]. Increasing this ratio moves the alloy deeper into the miscibility gap (indicated by a slower decomposition and a smaller correlation length); decreasing it moves it towards the miscibility line. A series of alloys, located along the tie-line between Vit1 and Vit4 (see table 1), also show systematic changes in the SANS results indicating that all alloys except Vit4 are inside the miscibility gap [73]. The Vit4 alloy does not show decomposition, and it appears to crystallize into spatially uncorrelated large crystals. The thermal stability of Vit4 in the SLS is higher than that of Vit1,

and no embrittlement upon annealing is observed as long as the sample is amorphous. This is the main reason that e.g. the golf club heads mentioned in section 2.3 are prepared from Vit4. This is a nice example of how systematic investigations of a material can lead to a better understanding of the synthesis–property–function relationship and to improvements in applications.

4. Summary

In summary, this paper gives a short overview on bulk metallic glasses and their properties. It deals with the Vitreloy™ alloys in more detail and reviews the current knowledge of their thermodynamic functions, TTT diagrams, atomic transport, and mechanical properties and closes with a section on decomposition and nanocrystallization in the Vit1 alloy, a phenomenon that is responsible for the limited thermal stability of this alloy against crystallization. The results of a detailed investigation suggest a strategy for improving the material.

Acknowledgments

The author gratefully acknowledges the continuous support of W L Johnson and K Samwer and fruitful collaborations with U Geyer, G Görigk, C C Hays, A Rehmet, M Seibt, and P Thiyagarajan.

References

[1] Klement W *et al* 1960 *Nature* **187** 869
[2] Buckel W and Hilsch R 1954 *Z. Phys.* **138** 109
[3] Drehman A J and Greer A L 1984 *Acta Metall.* **32** 323
[4] Inoue A, Othera K, Kita K and Masumoto T 1988 *Japan. J. Appl. Phys.* **27** L1799
[5] Inoue A, Zhang T and Masumoto T 1990 *Mater. Trans. JIM* **31** 177
[6] Inoue A 1995 *Mater. Trans. JIM* **36** 866
[7] Inoue A and Gook J 1995 *Mater. Trans. JIM* **36** 1180
[8] Inoue A and Gook J 1996 *Mater. Trans. JIM* **37** 32
[9] Inoue A and Katsuya A 1996 *Mater. Trans. JIM* **37** 1332
[10] Inoue A, Nishiyama N and Matsuda T 1996 *Mater. Trans. JIM* **37** 181
[11] Inoue A, Zhang T, Itoi T and Takeuchi A 1997 *Mater. Trans. JIM* **38** 359
[12] Peker A and Johnson W L 1993 *Appl. Phys. Lett.* **63** 2342
[13] Lin X H and Johnson W L 1995 *J. Appl. Phys.* **78** 6514
[14] Hays C, Kim C P and Johnson W 1999 *Appl. Phys. Lett.* **75** 1089
[15] Hays C C, Schroers J, Geyer U, Bossuyt S, Stein N and Johnson W L 2000 *Mater. Sci. Forum* **343** 103
[16] Turnbull D 1969 *Contemp. Phys.* **10** 473
[17] Turnbull D 1956 *Solid State Physics* vol 3 (New York: Academic) p 226
[18] Johnson W L 1999 *MRS Bull.* **24** 42
[19] Egami T and Waseda Y 1984 *J. Non-Cryst. Solids* **64** 113
[20] Greer A L 1993 *Nature* **366** 303
[21] Inoue A, Zhang T and Takeuchi A 1998 *Mater. Sci. Forum* **269–272** 855
[22] Desre P, Itami T and Ansara I 1993 *Z. Metallk.* **84** 185
[23] Desre P 1997 *Mater. Trans. JIM* **38** 583
[24] Desre P 1999 *Mater. Res. Soc. Symp. Proc.* **544** 51
[25] Busch R, Kim Y and Johnson W 1995 *J. Appl. Phys.* **77** 4093
[26] Busch R, Liu W and Johnson W 1998 *J. Appl. Phys.* **83** 4134
[27] Busch R, Kim Y J and Johnson W L 1995 *J. Appl. Phys.* **77** 4093
[28] Glade S C, Busch R, Lee D S and Johnson W L 2000 *J. Appl. Phys.* **87** 7242
[29] Ohsaka K, Chung S K, Rhim W K, Peker A, Scruggs D and Johnson W L 1997 *Appl. Phys. Lett.* **70** 726
[30] Samwer K, Busch R and Johnson W L 1999 *Phys. Rev. Lett.* **82** 580

[31] Rhim W K, Chung S K, Barber D, Man K F, Gutt G, Rulison A J and Spjut R E 1993 *Rev. Sci. Instrum.* **64** 2961
[32] Kim Y, Busch R, Johnson W, Rulison A and Rhim W 1996 *Appl. Phys. Lett.* **68** 1057
[33] Masuhr A, Waniuk T A, Busch R and Johnson W L 1999 *Phys. Rev. Lett.* **82** 2290
[34] Knorr K, Macht M-P, Freitag K and Mehrer H 1999 *J. Non-Cryst. Solids* **252** 669
[35] Masuhr A, Busch R and Johnson W 1998 *Mater. Sci. Forum, part 2* vol 269-2, p 779
[36] Masuhr A 1999 *PhD Thesis* California Institute of Technology
[37] Schroers J, Busch R, Masuhr A and Johnson W 1999 *J. Non-Cryst. Solids* **252** 699
[38] Schroers J, Busch R, Masuhr A and Johnson W 1999 *Appl. Phys. Lett.* **74** 2806
[39] Angell C A 1995 *Science* **267** 1924
[40] Turnbull D and Cohen M H 1961 *J. Chem. Phys.* **34** 120
[41] Leutheusser E 1984 *Phys. Rev.* A **29** 2765
Götze W and Sjögren L 1992 *Rep. Prog. Phys.* **55** 241
[42] Scherer G W 1993 *J. Am. Ceram. Soc.* **75** 1060
[43] Bakke E, Busch R and Johnson W L 1995 *Appl. Phys. Lett.* **67** 3260
[44] Busch R, Bakke E and Johnson W L 1998 *Acta Mater.* **46** 4725
[45] Masuhr A, Waniuk T A, Busch R and Johnson W L 1999 *Phys. Rev. Lett.* **82** 2290
[46] Grest G S and Cohen M H 1981 *Adv. Chem. Phys.* **48** 455
[47] Böhmer R, Ngai K L, Angell C A and Plazek D J 1993 *J. Chem. Phys.* **99** 4201
[48] Debenedetti P G 1996 *Metastable Liquids: Concepts and Principles* (Princeton, NJ: Princeton University Press)
[49] Perera D N 1999 *J. Phys.: Condens. Matter* **11** 3807
[50] Busch R, Masuhr A, Bakke E and Johnson W L 1997 *Mater. Res. Soc. Symp. Proc.* **455** 369
[51] Glade S C and Johnson W L 2000 *J. Appl. Phys.* **87** 7249
[52] Geyer U, Schneider S, Johnson W L, Qiu Y, Tombrello T A and Macht M-P 1995 *Phys. Rev. Lett.* **75** 2364
[53] Geyer U, Schneider S, Johnson W L, Qiu Y, Tombrello T A and Macht M-P 1996 *Appl. Phys. Lett.* **69** 2492
[54] Qiu Y, Geyer U, Schneider S, Macht M-P, Johnson W L and Tombrello T A 1996 *Nucl. Instrum. Methods* B **117** 151
[55] Budke E, Fielitz P, Macht M-P, Naundorf V and Frohberg G 1997 *Defect Diffus. Forum* **143** 825
[56] Ehmler H, Heesemann A, Rätzke K, Faupel F and Geyer U 1998 *Phys. Rev. Lett.* **80** 4919
[57] Tang X-P, Busch R, Johnson W L and Wu Y 1998 *Phys. Rev. Lett.* **81** 5358
[58] Tang X-P, Geyer U, Busch R, Johnson W L and Wu Y 1999 *Nature* **402** 160
[59] Ehmler H, Rätzke K and Faupel F 1998 *J. Non-Cryst. Solids* **252** 684
[60] Faupel F 1992 *Phys. Status Solidi* a **134** 9
[61] Schober H R, Gaukel C and Oligschleger C 1997 *Prog. Theor. Phys.* **126** 67
[62] Teichler H 1997 *Defect Diffus. Forum* **143** 717
[63] Donati C, Douglas J F, Kob W, Plimpton S J, Poole P H and Glotzer S C 1998 *Phys. Rev. Lett.* **80** 2338
[64] Meyer A, Wuttke J, Petry W, Randl O G and Schober H 1998 *Phys. Rev. Lett.* **80** 4454
[65] Götze W and Sjögren L 1995 *Transport Theory Stat. Phys.* **24** 801
[66] Frohberg G, Kraatz K H and Wever H 1987 *Mater. Sci. Forum* **15** 529
[67] Bruck H A, Rosakis A J and Johnson W L 1996 *J. Mater. Res.* **11** 503
[68] See http://www.liquidmetalgolf.com
[69] Gilbert C J, Ritchie R O and Johnson W L 1997 *Appl. Phys. Lett.* **71** 476
[70] Hays C C, Kim C P and Johnson W L 2000 *Phys. Rev. Lett.* **84** 2901
[71] Geyer U, Schneider S, Qiu Y, Macht M-P, Tombrello T A and Johnson W L 1996 *Mater. Sci. Forum* **225–227** 89
[72] Schneider S, Thiyagarajan P and Johnson W L 1996 *Appl. Phys. Lett.* **68** 493
[73] Schneider S *et al* unpublished
[74] Schneider S, Geyer U, Thiyagarajan P and Johnson W L 1997 *Mater. Sci. Forum* **235–238** 337
[75] Schneider S, Geyer U, Thiyagarajan P, Busch R, Schulz R, Samwer K and Johnson W L 1996 *Mater. Sci. Forum* **225–227** 59
[76] Busch R, Schneider S, Peker A and Johnson W L 1995 *Appl. Phys. Lett.* **67** 1544
[77] Cahn J W and Hilliard J E 1958 *J. Chem. Phys.* **28** 258
[78] Cahn J W and Hilliard J E 1959 *J. Chem. Phys.* **31** 688
[79] Kelton K F 1998 *Phil. Mag. Lett.* **77** 337
[80] Hermann H, Wiedenmann A and Uebele P 1998 *Physica* B **241–243** 352
[81] Löffler J and Johnson W L 2000 *Appl. Phys. Lett.* **76** 3394
[82] Schneider S, Thiyagarajan P, Geyer U and Johnson W L 1997 *Physica* B **241** 918